

Supporting Information

Reversible on–off switching of a single-chain magnet via single-crystal-to-single-crystal transition- and light-induced metal-to-metal electron transfer

Meng-Jia Shang,^a Han-Han Lu,^a Qiang Liu,^b Ren-He Zhou,^a Hui-Ying Sun^a, Zhen Shao,^a Yin-Shan Meng^{*a} and Tao Liu^{*a}

^a *State Key Laboratory of Fine Chemicals, Frontier Science Center for Smart Materials, School of Chemical Engineering, Dalian University of Technology, 2 Linggong Road, Dalian 116024, China.*

^b *Instrumental Analysis Center, Dalian University of Technology, 2 Linggong Road, Dalian 116024, China*

*Corresponding Author(s): mengys@dlut.edu.cn (Y.-S. Meng); liutao@dlut.edu.cn (T. Liu)

Contents

Table S1. Crystallographic Data for 1·solv , 1·desolv and 1·resolv at 298 K.	3
Table S2. Crystallographic Data for 1·solv at 60 K before and after 808- and 532-nm light irradiations.	4
Table S3. Selected bond distances (Å) and angles (°) for 1·solv at 298 K.	5
Table S4. Selected bond distances (Å) and angles (°) for 1·desolv at 298 K.	6
Table S5. Selected bond distances (Å) and angles (°) for 1·resolv at 298 K.	7
Table S6. Selected bond distances (Å) and angles (°) for 1·solv at 60 K.	8
Table S7. Selected bond distances (Å) and angles (°) for 1·solv after 808 nm irradiation at 60 K. ...	9
Table S8. Selected bond distances (Å) and angles (°) for 1·solv after 532 nm irradiation at 60 K. .	10
Table S9. Continuous Shape Measure (CShM) analyses of geometries for compounds 1·solv and 1·desolv at 298 K by SHAPE 2.0 Software.	11
Table S10. Hydrogen bond distances (Å) and angles (°) for 1·solv at 298 K.	11
Table S11. ⁵⁷ Fe Mössbauer parameters for 1·solv at 200 K.	12
Table S12. Temperature-dependent ⁵⁷ Fe Mössbauer parameters for 1·desolv	12
Fig. S1. TGA analyses of 1·solv in the nitrogen atmosphere at 10 K min ⁻¹	13
Fig. S2. Schematic structures of the {Fe ₂ Co}-based double zig-zag chains in 1·desolv at 298 K. ...	13
Fig. S3. The overlapped molecular structures of 1·solv and 1·desolv at 298 K.	14
Fig. S4. Crystal structure of 1·resolv at 298 K.	14
Fig. S5. The simulated and experimental powder X-ray diffraction patterns of 1·solv at 298 K.	15
Fig. S6. Plots of χT vs T for 1·solv between 2 and 300 K.	15
Fig. S7 Temperature dependent ⁵⁷ Fe Mössbauer spectra of 1·solv at 200 K.	16
Fig. S8. Infrared spectra for compounds 1·solv and 1·desolv at 298 K.	16
Fig. S9. Solid state UV-vis-NIR spectra for 1·solv and 1·desolv at 298 K.	17
Fig. S10. Plots of χT vs time for 1·solv irradiated under 808 nm at 10 K.	17
Fig. S11. Temperature-dependent susceptibilities of 1·solv before and after light irradiation under an 1000 Oe DC field.	18
Fig. S12. Arrhenius plots for the magnetic relaxation process of 1·solv after 808 nm light irradiation based on the peak values of χ''	18
Fig. S13. Hydrogen bonds formed between lattice solvent molecules and terminal cyanide nitrogen atoms for 1·solv	19
Fig. S14. Variable temperature solid state IR spectra of 1·desolv in cooling mode.	19
Fig. S15. Variable temperature solid state UV-vis-NIR absorption spectra of 1·desolv in cooling mode.	20
Fig. S16. Temperature dependence of in-phase signals (χ') (a) and out-of-phase signals (χ'') (b) for 1·desolv under a 5 Oe AC field and 2000 Oe DC field.	21
Fig. S17. Plots of χT vs. T for 1·resolv between 2 and 300 K.	22

Table S1. Crystallographic Data for **1·solv**, **1·desolv** and **1·resolv** at 298 K.

	1·solv	1·desolv	1·resolv
Formula	C ₅₀ H ₄₇ B ₂ CoFe ₂ I ₂ N ₂₆ O _{2.5}	C ₄₈ H ₃₈ B ₂ CoFe ₂ I ₂ N ₂₆	C ₄₉ H ₄₄ B ₂ CoFe ₂ I ₂ N ₂₆ O ₂
Fw	1498.19	1425.09	1475.15
Crystal system	Triclinic	Triclinic	Triclinic
Space group	<i>P</i> $\bar{1}$	<i>P</i> $\bar{1}$	<i>P</i> $\bar{1}$
<i>a</i> , Å	13.3825(4)	13.401(4)	13.445(3)
<i>b</i> , Å	13.8767(4)	13.567(5)	13.530(3)
<i>c</i> , Å	17.8617(5)	18.266(6)	17.944(4)
α , °	79.1420(10)	70.833(9)	78.456(6)
β , °	70.1710(10)	78.105(9)	70.117(6)
γ , °	77.3290(10)	75.770(9)	76.611(6)
<i>V</i> , Å ³	3020.78(15)	3011.8(17)	2959.9(10)
<i>Z</i>	1	2	2
ρ_{calc} , g/cm ³	1.647	1.571	1.655
μ /mm ⁻¹	1.831	1.829	1.867
<i>F</i> (000)	1488.0	1406.0	1462.0
Reflections collected	65667	45629	57552
Unique reflections (<i>R</i> _{int})	0.0353	0.1805	0.0791
Goodness-of-fit on <i>F</i> ²	1.028	1.024	1.061
<i>R</i> ₁ , [<i>I</i> >2 σ (<i>I</i>)]	0.0428	0.0977	0.0633
<i>wR</i> ₂ , [<i>I</i> >2 σ (<i>I</i>)]	0.0963	0.2152	0.1720

$$R_1 = \Sigma (|F_o| - |F_c|) / \Sigma |F_o|, \quad wR_2 = \{\Sigma [w(F_o^2 - F_c^2)^2] / \Sigma [w(F_o^2)^2]\}^{1/2}$$

Table S2. Crystallographic Data for **1·solv** at 60 K before and after 808- and 532-nm light irradiations.

	1·solv	1·solv ^{808 nm}	1·solv ^{532 nm}
Formula	C ₅₀ H ₄₇ B ₂ CoFe ₂ I ₂ N ₂₆ O _{2.5}	C ₅₀ H ₄₇ B ₂ CoFe ₂ I ₂ N ₂₆ O _{2.5}	C ₅₀ H ₄₇ B ₂ CoFe ₂ I ₂ N ₂₆ O _{2.5}
<i>F</i> w	1498.19	1498.19	1498.19
Crystal system	Triclinic	Triclinic	Triclinic
Space group	<i>P</i> $\bar{1}$	<i>P</i> $\bar{1}$	<i>P</i> $\bar{1}$
<i>a</i> , Å	13.321(1)	13.365(2)	13.343(1)
<i>b</i> , Å	13.574(0)	13.654(2)	13.538(1)
<i>c</i> , Å	17.762(5)	18.330(3)	17.779(4)
α , °	78.044(3)	78.405(4)	78.010(2)
β , °	70.353(4)	70.864(5)	70.254(2)
γ , °	76.573(3)	75.394(5)	76.594(2)
<i>V</i> , Å ³	2912.8(5)	3032.1(8)	2911.0(4)
<i>Z</i>	1	1	1
ρ_{calc} , g/cm ³	1.708	1.641	1.709
μ /mm ⁻¹	1.899	1.824	1.900
<i>F</i> (000)	1488.0	1488.0	1488.0
Reflections collected	17349	44099	43980
Unique reflections (<i>R</i> _{int})	0.0853	0.1066	0.1270
Goodness-of-fit on <i>F</i> ²	1.021	1.013	1.021
<i>R</i> ₁ , [<i>I</i> > 2σ(<i>I</i>)]	0.0676	0.0777	0.0611
<i>wR</i> ₂ , [<i>I</i> > 2σ(<i>I</i>)]	0.1603	0.1882	0.1024

$$R_1 = \Sigma (|F_o| - |F_c|) / \Sigma |F_o|, \quad wR_2 = \{ \Sigma [w(F_o^2 - F_c^2)^2] / \Sigma [w(F_o^2)^2] \}^{1/2}$$

Table S3. Selected bond distances (Å) and angles (°) for **1·solv** at 298 K.

Bond length (Å)		Bond angle (°)	
Co(1)–N(3)	1.882(3)	N(5)#1–Co(1)–N(7)	89.92(11)
Co(1)–N(3)#1	1.882(3)	N(5)–Co(1)–N(7)#1	89.92(11)
Co(1)–N(5)	1.876(3)	N(5)–Co(1)–N(7)	90.08(11)
Co(1)–N(5)#1	1.876(3)	N(5)#1–Co(1)–N(7)#1	90.08(11)
Co(1)–N(7)	1.940(3)	N(5)–Co(1)–N(3)	89.59(11)
Co(1)–N(7)#1	1.940(3)	N(5)–Co(1)–N(3)#1	90.41(11)
Co(2)–N(2)	1.891(3)	N(5)#1–Co(1)–N(3)#1	89.59(11)
Co(2)–N(2)#2	1.891(3)	N(5)#1–Co(1)–N(3)	90.41(11)
Co(2)–N(6)	1.887(3)	N(3)–Co(1)–N(7)	91.70(11)
Co(2)–N(6)#2	1.887(3)	N(3)–Co(1)–N(7)#1	88.30(11)
Co(2)–N(8)	1.947(3)	N(3)#1–Co(1)–N(7)#1	91.70(11)
Co(2)–N(8)#2	1.947(3)	N(3)#1–Co(1)–N(7)	88.30(11)
Fe(1)–C(1)	1.917(4)	N(6)#2–Co(2)–N(8)	90.13(11)
Fe(1)–C(2)	1.916(4)	N(6)–Co(2)–N(8)#2	90.13(11)
Fe(1)–C(3)	1.912(3)	N(6)–Co(2)–N(8)	89.87(11)
Fe(1)–N(14)	1.969(3)	N(6)#2–Co(2)–N(8)#2	89.87(11)
Fe(1)–N(16)	1.956(3)	N(6)–Co(2)–N(2)	89.36(11)
Fe(1)–N(18)	1.969(3)	N(6)#2–Co(2)–N(2)#2	89.36(11)
Fe(2)–C(4)	1.912(4)	N(6)#2–Co(2)–N(2)	90.64(11)
Fe(2)–C(5)	1.861(3)	N(6)–Co(2)–N(2)#2	90.64(11)
Fe(2)–C(6)	1.866(3)	N(2)–Co(2)–N(8)#2	89.51(11)
Fe(2)–N(22)	2.003(2)	N(2)#2–Co(2)–N(8)#2	90.49(11)
Fe(2)–C(24)	2.014(3)	N(2)–Co(2)–N(8)	90.49(11)
Fe(2)–N(26)	1.991(2)	N(2)#2–Co(2)–N(8)	89.51(11)

#1 1-X, 1-Y, 1-Z; #2 -X, 1-Y, 1-Z

Table S4. Selected bond distances (Å) and angles (°) for **1·desolv** at 298 K.

Bond length (Å)		Bond angle (°)	
Co(1)–N(3)	2.076(10)	N(5)#1–Co(1)–N(7)	92.1(3)
Co(1)–N(3)#1	2.076(10)	N(5)–Co(1)–N(7)	87.9(4)
Co(1)–N(5)	2.072(9)	N(5)#1–Co(1)–N(7)#1	87.9(4)
Co(1)–N(5)#1	2.072(9)	N(5)–Co(1)–N(7)#1	92.1(3)
Co(1)–N(7)	2.127(9)	N(5)–Co(1)–N(3)#1	87.9(4)
Co(1)–N(7)#1	2.127(9)	N(5)–Co(1)–N(3)	92.1(4)
Co(2)–N(2)	2.093(8)	N(5)#1–Co(1)–N(3)#1	92.1(4)
Co(2)–N(2)#2	2.093(8)	N(5)#1–Co(1)–N(3)	87.9(4)
Co(2)–N(6)	2.058(9)	N(3)–Co(1)–N(7)	90.6(4)
Co(2)–N(6)#2	2.058(9)	N(3)–Co(1)–N(7)#1	89.4(4)
Co(2)–N(8)	2.124(8)	N(3)#1–Co(1)–N(7)	89.4(4)
Co(2)–N(8)#2	2.124(8)	N(3)#1–Co(1)–N(7)#1	90.6(4)
Fe(1)–C(1)	1.919(13)	N(2)–Co(2)–N(8)#2	90.4(3)
Fe(1)–C(2)	1.886(10)	N(2)#2–Co(2)–N(8)	90.4(3)
Fe(1)–C(3)	1.884(10)	N(2)–Co(2)–N(8)	89.6(3)
Fe(1)–N(14)	1.958(8)	N(2)#2–Co(2)–N(8)#2	89.6(3)
Fe(1)–N(16)	1.949(8)	N(6)#2–Co(2)–N(2)	89.6(3)
Fe(1)–N(18)	1.974(8)	N(6)#2–Co(2)–N(2)#2	90.4(3)
Fe(2)–C(4)	1.916(13)	N(6)–Co(2)–N(2)#2	89.6(3)
Fe(2)–C(5)	1.882(11)	N(6)–Co(2)–N(2)	90.4(3)
Fe(2)–C(6)	1.898(12)	N(6)–Co(2)–N(8)	89.7(4)
Fe(2)–N(22)	1.972(9)	N(6)#2–Co(2)–N(8)#2	89.7(4)
Fe(2)–C(24)	1.972(8)	N(6)#2–Co(2)–N(8)	90.3(4)
Fe(2)–N(26)	1.961(8)	N(6)–Co(2)–N(8)#2	90.3(4)

#1 1-X, 1-Y, 1-Z; #2 1-X, 2-Y, 1-Z

Table S5. Selected bond distances (Å) and angles (°) for **1·resolv** at 298 K.

Bond length (Å)		Bond angle (°)	
Co(1)–N(3)	1.871(7)	N(5)#1–Co(1)–N(7)	89.7(2)
Co(1)–N(3)#2	1.872(7)	N(5)#3–Co(1)–N(7)#2	89.7(2)
Co(1)–N(5)#1	1.891(6)	N(5)#1–Co(1)–N(7)#2	90.3(2)
Co(1)–N(5)#3	1.891(6)	N(5)#3–Co(1)–N(7)	90.3(2)
Co(1)–N(7)	1.951(6)	N(3)–Co(1)–N(7)	91.1(3)
Co(1)–N(7)#2	1.951(6)	N(3)–Co(1)–N(7)#2	88.9(3)
Co(2)–N(2)	1.887(6)	N(3)#2–Co(1)–N(7)	88.9(3)
Co(2)–N(2)#1	1.887(6)	N(3)#2–Co(1)–N(7)#2	91.1(3)
Co(2)–N(6)	1.873(7)	N(3)–Co(1)–N(5)#1	88.7(3)
Co(2)–N(6)#1	1.874(7)	N(3)#2–Co(1)–N(5)#1	91.3(3)
Co(2)–N(8)	1.953(6)	N(3)#2–Co(1)–N(5)#3	88.7(3)
Co(2)–N(8)#1	1.953(6)	N(3)–Co(1)–N(5)#3	91.3(3)
Fe(1)–C(1)	1.914(9)	N(2)–Co(2)–N(8)	89.0(2)
Fe(1)–C(2)	1.860(7)	N(2)–Co(2)–N(8)#1	91.0(2)
Fe(1)–C(3)	1.854(8)	N(2)#1–Co(2)–N(8)#1	89.0(2)
Fe(1)–N(14)	1.997(6)	N(2)#1–Co(2)–N(8)	91.0(2)
Fe(1)–N(16)	1.981(6)	N(6)#1–Co(2)–N(8)	90.0(3)
Fe(1)–N(18)	2.013(6)	N(6)#1–Co(2)–N(8)#1	90.0(3)
Fe(2)–C(4)	1.932(9)	N(6)–Co(2)–N(8)	90.0(3)
Fe(2)–C(5)	1.907(8)	N(6)–Co(2)–N(8)#1	90.0(3)
Fe(2)–C(6)	1.895(9)	N(6)–Co(2)–N(2)	90.3(3)
Fe(2)–N(22)	1.969(6)	N(6)#1–Co(2)–N(2)#1	90.3(3)
Fe(2)–C(24)	1.950(6)	N(6)#1–Co(2)–N(2)	89.7(3)
Fe(2)–N(26)	1.970(6)	N(6)–Co(2)–N(2)#1	89.7(3)

#1 1-X,1-Y,1-Z; #2 -X,1-Y,1-Z; #3 -1+X,+Y,+Z

Table S6. Selected bond distances (Å) and angles (°) for **1·solv** at 60 K.

Bond length (Å)		Bond angle (°)	
Co(1)–N(3)	1.888(7)	N(3)–Co(1)–N(5)#1	89.7(3)
Co(1)–N(3)#1	1.888(7)	N(3)#1–Co(1)–N(5)#1	90.3(3)
Co(1)–N(5)	1.893(7)	N(3)#1–Co(1)–N(5)	89.7(3)
Co(1)–N(5)#1	1.893(7)	N(3)–Co(1)–N(5)	90.3(3)
Co(1)–N(7)	1.942(7)	N(3)–Co(1)–N(7)#1	90.0(3)
Co(1)–N(7)#1	1.942(7)	N(3)#1–Co(1)–N(7)	90.0(3)
Co(2)–N(2)	1.868(7)	N(3)#1–Co(1)–N(7)#1	90.0(3)
Co(2)–N(2)#2	1.868(7)	N(3)–Co(1)–N(7)	90.0(3)
Co(2)–N(6)#1	1.882(7)	N(5)#1–Co(1)–N(7)	90.3(3)
Co(2)–N(6)#3	1.882(7)	N(5)–Co(1)–N(7)	89.7(3)
Co(2)–N(8)	1.935(7)	N(5)#1–Co(1)–N(7)#1	89.7(3)
Co(2)–N(8)#2	1.935(7)	N(5)–Co(1)–N(7)#1	90.3(3)
Fe(1)–C(1)	1.912(9)	N(6)#3–Co(2)–N(8)	89.1(3)
Fe(1)–C(2)	1.866(9)	N(6)#1–Co(2)–N(8)#2	89.1(3)
Fe(1)–C(3)	1.860(8)	N(6)#3–Co(2)–N(8)#2	90.9(3)
Fe(1)–N(14)	1.999(6)	N(6)#1–Co(2)–N(8)	90.9(3)
Fe(1)–N(16)	2.018(7)	N(2)–Co(2)–N(6)#3	90.1(3)
Fe(1)–N(18)	1.993(6)	N(2)–Co(2)–N(6)#1	89.9(3)
Fe(2)–C(4)	1.931(1)	N(2)#2–Co(2)–N(6)#3	89.9(3)
Fe(2)–C(5)	1.921(9)	N(2)#2–Co(2)–N(6)#1	90.1(3)
Fe(2)–C(6)	1.917(9)	N(2)–Co(2)–N(8)	89.9(3)
Fe(2)–N(22)	1.982(6)	N(2)–Co(2)–N(8)#2	90.1(3)
Fe(2)–N(24)	1.945(7)	N(2)#2–Co(2)–N(8)	90.1(3)
Fe(2)–N(26)	1.973(7)	N(2)#2–Co(2)–N(8)#2	89.9(3)

#1 1-X,1-Y,1-Z; #2 2-X,1-Y,1-Z; #3 1+X,+Y,+Z

Table S7. Selected bond distances (Å) and angles (°) for **1·solv** after 808 nm irradiation at 60 K.

Bond length (Å)	808 nm-irradiated	Bond angle (°)	808 nm-irradiated
Co(1)–N(3)	2.073(8)	N(5)#1–Co(1)–N(7)#1	91.1(4)
Co(1)–N(3)#1	2.073(9)	N(5)–Co(1)–N(7)#1	88.9(4)
Co(1)–N(5)	2.096(1)	N(5)#1–Co(1)–N(7)	88.9(4)
Co(1)–N(5)#1	2.096(1)	N(5)–Co(1)–N(7)	91.1(4)
Co(1)–N(7)	2.129(8)	N(3)#1–Co(1)–N(5)#1	93.2(4)
Co(1)–N(7)#1	2.129(8)	N(3)–Co(1)–N(5)	93.2(4)
Co(2)–N(2)	2.111(12)	N(3)–Co(1)–N(5)#1	86.8(4)
Co(2)–N(2)#2	2.111(12)	N(3)#1–Co(1)–N(5)	86.8(4)
Co(2)–N(6)	2.083(8)	N(3)–Co(1)–N(7)#1	87.1(3)
Co(2)–N(6)#2	2.083(8)	N(3)#1–Co(1)–N(7)	87.1(3)
Co(2)–N(8)	2.130(8)	N(3)#1–Co(1)–N(7)#1	92.9(3)
Co(2)–N(8)#2	2.130(8)	N(3)–Co(1)–N(7)	92.9(3)
Fe(1)–C(1)	1.921(11)	N(2)–Co(2)–N(8)#2	90.1(3)
Fe(1)–C(2)	1.921(14)	N(2)#2–Co(2)–N(8)#2	89.9(3)
Fe(1)–C(3)	1.911(1)	N(2)–Co(2)–N(8)	89.9(3)
Fe(1)–N(14)	1.976(8)	N(2)#2–Co(2)–N(8)	90.1(3)
Fe(1)–N(16)	1.964(11)	N(6)#2–Co(2)–N(2)	88.4(3)
Fe(1)–N(18)	1.998(8)	N(6)–Co(2)–N(2)	91.6(3)
Fe(2)–C(4)	1.940(10)	N(6)#2–Co(2)–N(2)#2	91.6(3)
Fe(2)–C(5)	1.883(12)	N(6)–Co(2)–N(2)#2	88.4(3)
Fe(2)–C(6)	1.907(1)	N(6)#2–Co(2)–N(8)	89.7(3)
Fe(2)–N(22)	1.966(8)	N(6)–Co(2)–N(8)#2	89.7(3)
Fe(2)–C(24)	1.972(7)	N(6)#2–Co(2)–N(8)#2	90.3(3)
Fe(2)–N(26)	1.960(1)	N(6)–Co(2)–N(8)	90.3(3)

#1 2-X,1-Y,1-Z;#2 1-X,1-Y,1-Z

Table S8. Selected bond distances (Å) and angles (°) for **1·solv** after 532 nm irradiation at 60 K.

Bond length (Å)	532 nm-irradiated	Bond angle (°)	532 nm-irradiated
Co(1)–N(3)	1.887(6)	N(5)–Co(1)–N(7)	90.0(3)
Co(1)–N(3)#1	1.887(6)	N(5)#1–Co(1)–N(7)	90.0(3)
Co(1)–N(5)	1.894(7)	N(5)#1–Co(1)–N(7)#1	90.0(3)
Co(1)–N(5)#1	1.894(7)	N(5)–Co(1)–N(7)#1	90.0(3)
Co(1)–N(7)	1.944(6)	N(3)–Co(1)–N(7)#1	90.3(2)
Co(1)–N(7)#1	1.944(6)	N(3)#1–Co(1)–N(7)	90.3(2)
Co(2)–N(2)	1.881(7)	N(3)#1–Co(1)–N(7)#1	89.7(2)
Co(2)–N(2)#2	1.881(7)	N(3)–Co(1)–N(7)	89.7(2)
Co(2)–N(6)	1.885(6)	N(3)#1–Co(1)–N(5)	90.5(3)
Co(2)–N(6)#2	1.885(6)	N(3)#1–Co(1)–N(5)#1	89.5(3)
Co(2)–N(8)	1.932(6)	N(3)–Co(1)–N(5)	89.5(3)
Co(2)–N(8)#2	1.931(6)	N(3)–Co(1)–N(5)#1	90.5(3)
Fe(1)–C(1)	1.906(8)	N(2)#2–Co(2)–N(8)#2	90.1(3)
Fe(1)–C(2)	1.850(8)	N(2)–Co(2)–N(8)	90.1(3)
Fe(1)–C(3)	1.861(8)	N(2)–Co(2)–N(8)#2	89.9(2)
Fe(1)–N(14)	1.979(6)	N(2)#2–Co(2)–N(8)	89.9(2)
Fe(1)–N(16)	2.000(6)	N(2)–Co(2)–N(6)	90.1(3)
Fe(1)–N(18)	2.015(6)	N(2)–Co(2)–N(6)#2	89.9(3)
Fe(2)–C(4)	1.920(8)	N(2)#2–Co(2)–N(6)#2	90.1(3)
Fe(2)–C(5)	1.908(8)	N(2)#2–Co(2)–N(6)	89.9(3)
Fe(2)–C(6)#2	1.918(8)	N(6)–Co(2)–N(8)	88.8(2)
Fe(2)–N(22)	1.937(7)	N(6)–Co(2)–N(8)#2	91.2(2)
Fe(2)–C(24)	1.975(6)	N(6)#2–Co(2)–N(8)	91.2(2)
Fe(2)–N(26)	1.970(6)	N(6)#2–Co(2)–N(8)#2	88.8(2)

#1 1-X,1-Y,1-Z; #2 2-X,1-Y,1-Z

Table S9. Continuous Shape Measure (CShM) analyses of geometries for compounds **1·solv** and **1·desolv** at 298 K by SHAPE 2.0 Software.

Geometry	1·solv				1·desolv			
	Co1	Co2	Fe1	Fe2	Co1	Co2	Fe1	Fe2
Hexagon/ D_{6h}	32.557	32.849	32.157	32.340	31.985	32.890	32.438	32.169
Pentagonal pyramid/ C_{5v}	29.914	30.041	29.211	29.347	29.624	29.986	29.418	29.017
Octahedron/ O_h	0.039	0.023	0.074	0.153	0.059	0.019	0.090	0.131
Trigonal prism/ D_{3h}	16.507	16.639	15.599	15.647	16.223	16.678	16.136	15.714
Johnson pentagonal pyramid (J_2)/ C_{5v}	33.351	33.500	32.784	32.950	33.000	33.400	33.014	32.633

CShM: the continuous shape measurement relative to the ideal octahedron of the M centers, zero value means the ideal octahedron geometries.

Table S10. Hydrogen bond distances (Å) and angles (°) for **1·solv** at 298 K.

D–H⋯A	d(D–H)/ Å	d(H⋯A)/ Å	d(D–H⋯A)/ Å	D–H⋯A/ °
O1–H1A⋯N1	0.85	2.15	2.951(12)	156
O2–H18⋯N4	0.82	2.00	2.809(8)	172

Table S11. ^{57}Fe Mössbauer parameters for **1·solv** at 200 K.

T (K)	δ (mm s $^{-1}$)	ΔE_Q (mm s $^{-1}$)	Relative area (%)	Approximation ratio	Fe type
200K	0.23	0.65	50.96	1	Fe $^{\text{II}}_{\text{LS}}$
	-0.07	0.94	49.04	1	Fe $^{\text{III}}_{\text{LS}}$

Table S12. Temperature-dependent ^{57}Fe Mössbauer parameters for **1·desolv**.

T (K)	δ (mm s $^{-1}$)	ΔE_Q (mm s $^{-1}$)	Relative area (%)	Approximation ratio	Fe type
298K	-0.10	1.04	100	---	Fe $^{\text{III}}_{\text{LS}}$
80K	0.14	0.54	32.73	1	Fe $^{\text{II}}_{\text{LS}}$
	-0.01	1.41	67.27	1	Fe $^{\text{III}}_{\text{LS}}$

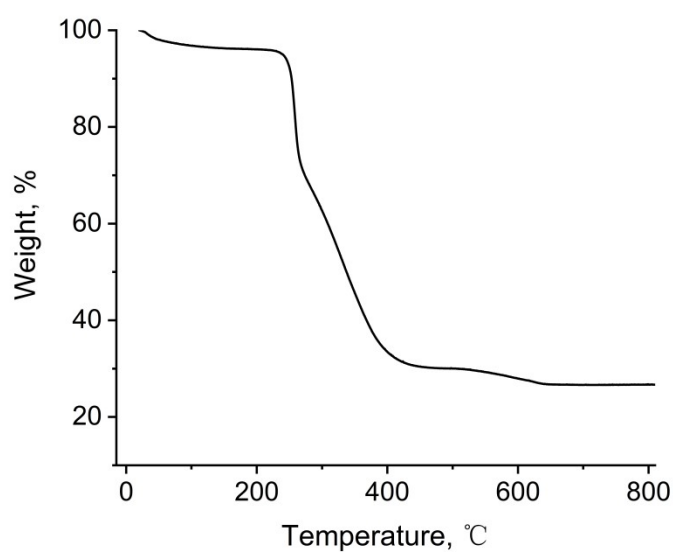


Fig. S1. TGA analyses of **1·solv** in the nitrogen atmosphere at 10 K min^{-1} . The first weight loss below $230 \text{ }^\circ\text{C}$ (experimental: 5.31% for **1·solv**) should be ascribed to the loss of isolated solvent molecules (expected: 5.48% for **1·solv**).

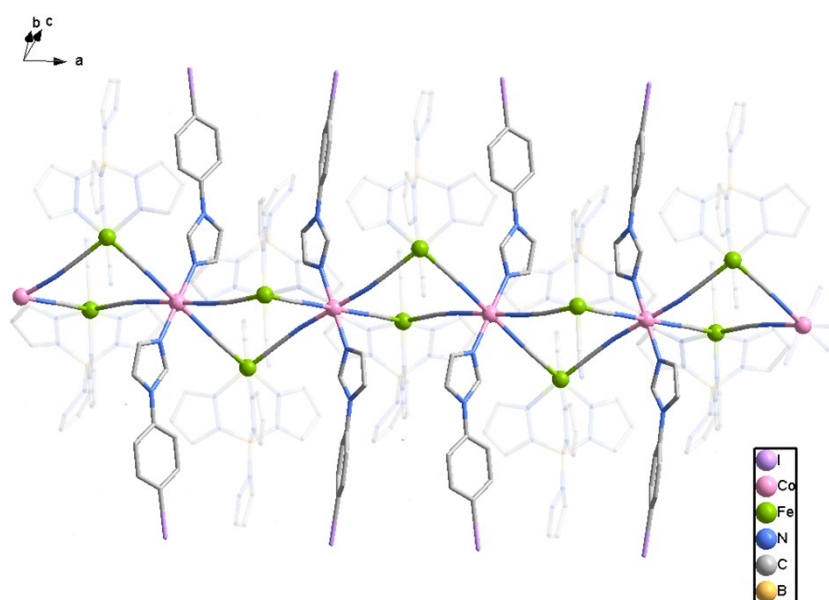


Fig. S2. Schematic structures of the $\{\text{Fe}_2\text{Co}\}$ -based double zig-zag chains in **1·desolv** at 298 K. H atoms have been omitted for clarity. Color code: Co, pink; Fe, green; B, yellow; C, grey; N, blue; I, purple.

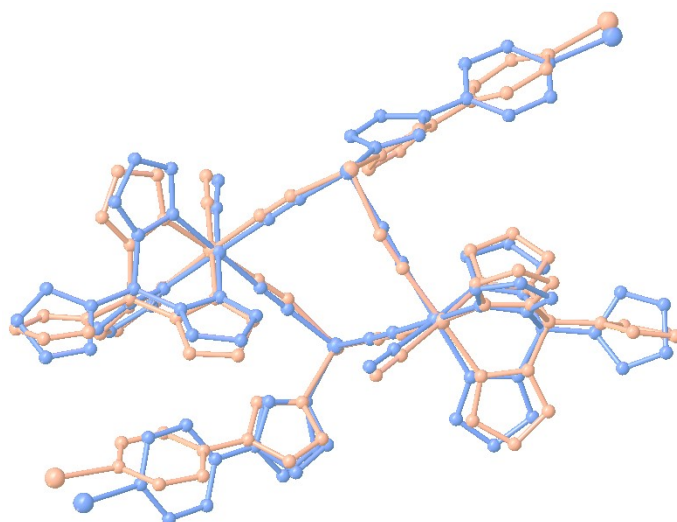


Fig S3. The overlapped molecular structures of **1·solv** (pale blue) and **1·desolv** (pale orange) at 298 K. Hydrogen atoms and solvents are omitted for clarity.

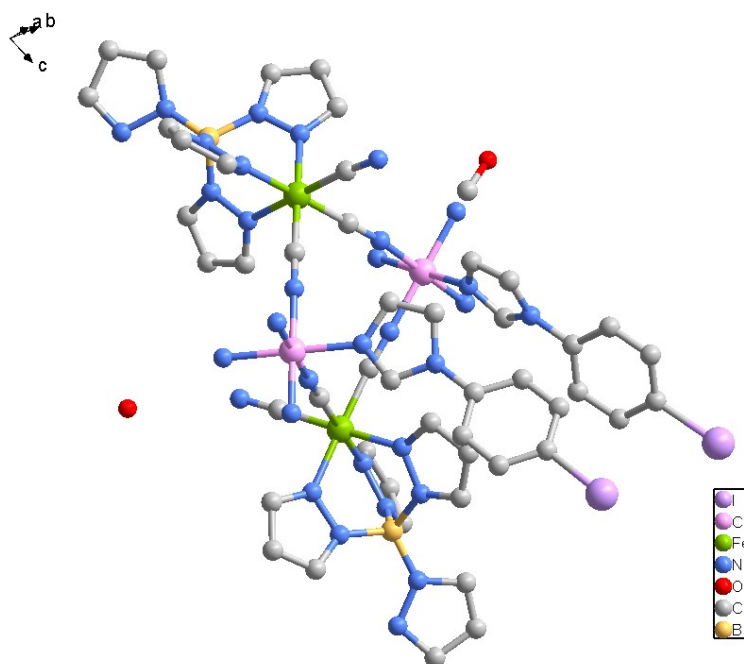


Fig. S4. Crystal structure of **1·resolv** at 298 K. H atoms have been omitted for clarity. Color code: Co, pink; Fe, green; B, yellow; C, grey; N, blue; O, red; I, purple.

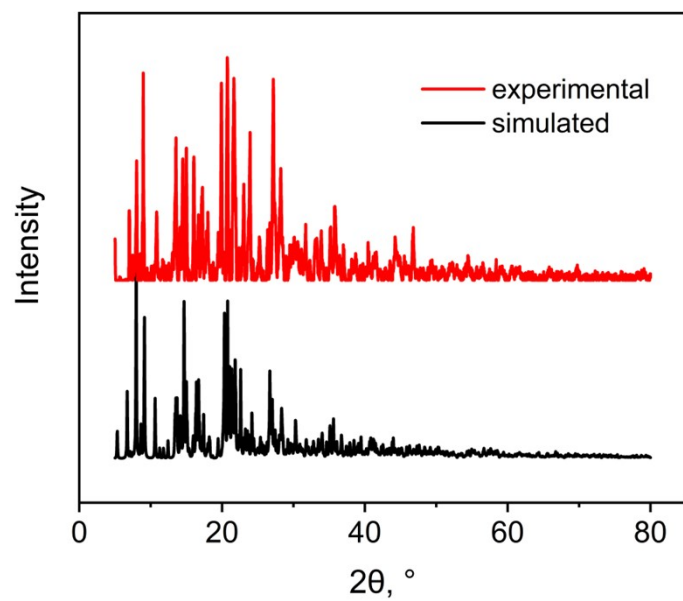


Fig. S5. The simulated and experimental powder X-ray diffraction patterns of $1 \cdot \text{solv}$ at 298 K.

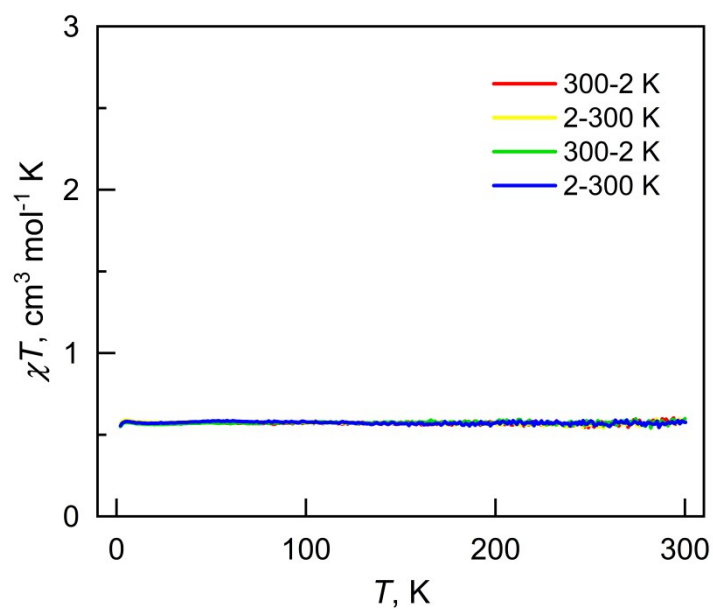


Fig. S6. Plots of χT vs T for $1 \cdot \text{solv}$ between 2 and 300 K.

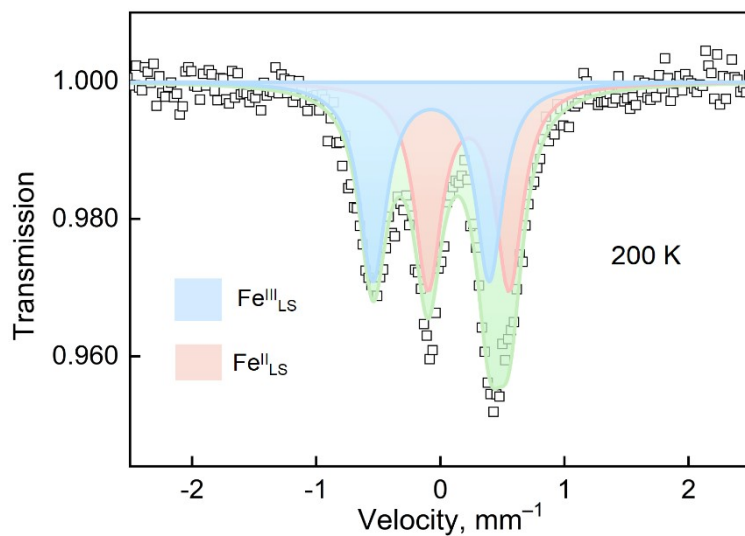


Fig. S7 Temperature dependent ^{57}Fe Mössbauer spectra of **1·solv** at 200 K. All spectra were fitted to Lorentzian profiles by the least-squares method, and the fit quality was controlled by the standard χ^2 and misfit tests (MossWinn program).

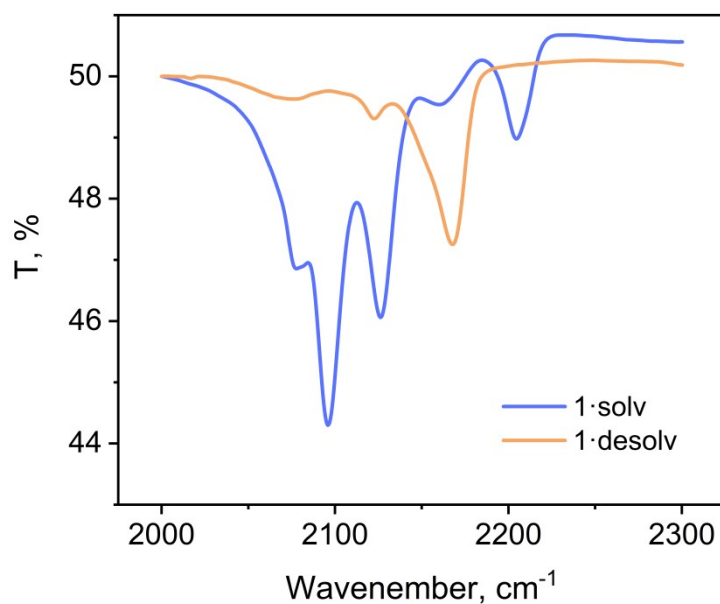


Fig. S8. Infrared spectra for compounds **1·solv** and **1·desolv** at 298 K

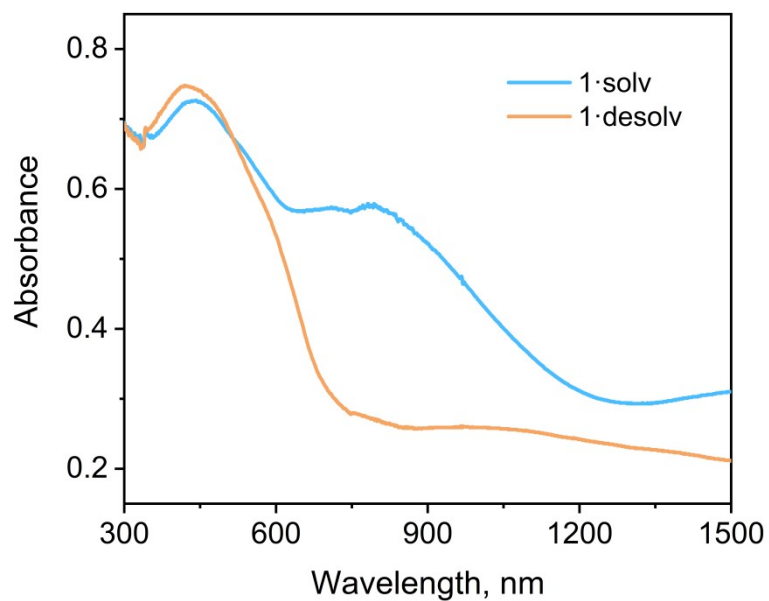


Fig. S9. Solid state UV-vis-NIR spectra for **1·solv** and **1·desolv** at 298 K.

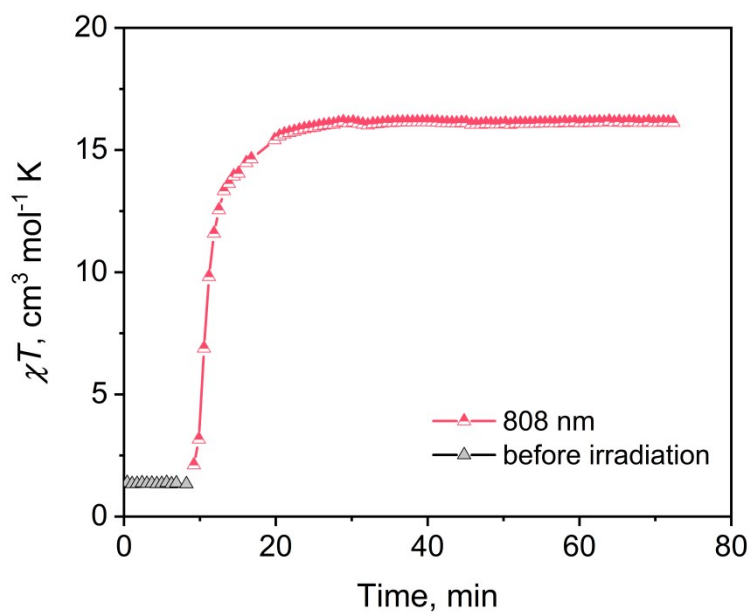


Fig. S10. Plots of χT vs time for **1·solv** irradiated under 808 nm at 10 K.

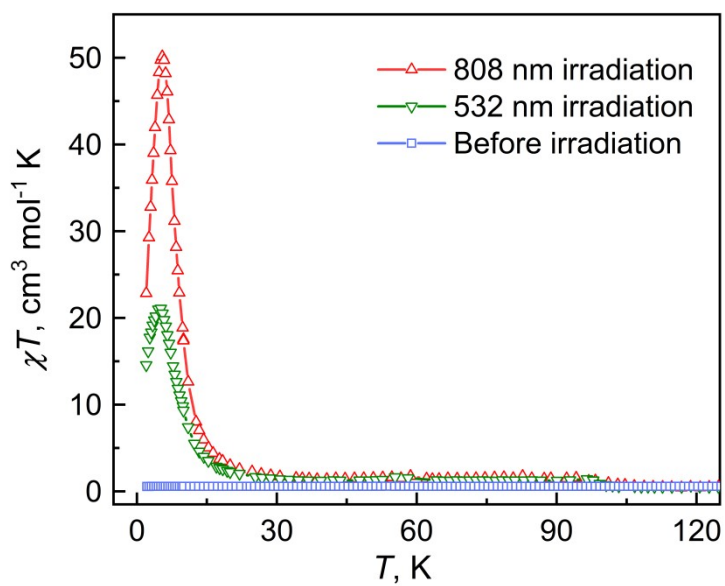


Fig. S11. Temperature-dependent susceptibilities of **1·solv** before and after light irradiation under an 1000 Oe DC field.

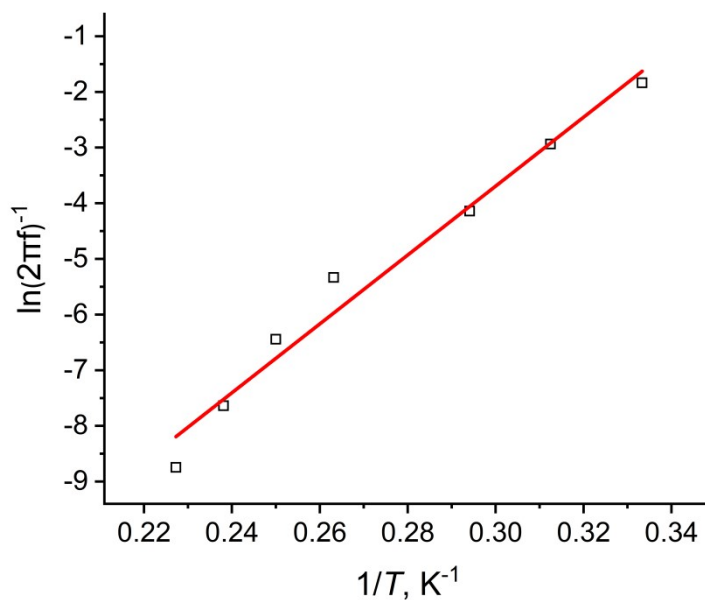


Fig. S12. Arrhenius plots for the magnetic relaxation process of **1·solv** after 808 nm light irradiation based on the peak values of χ'' .

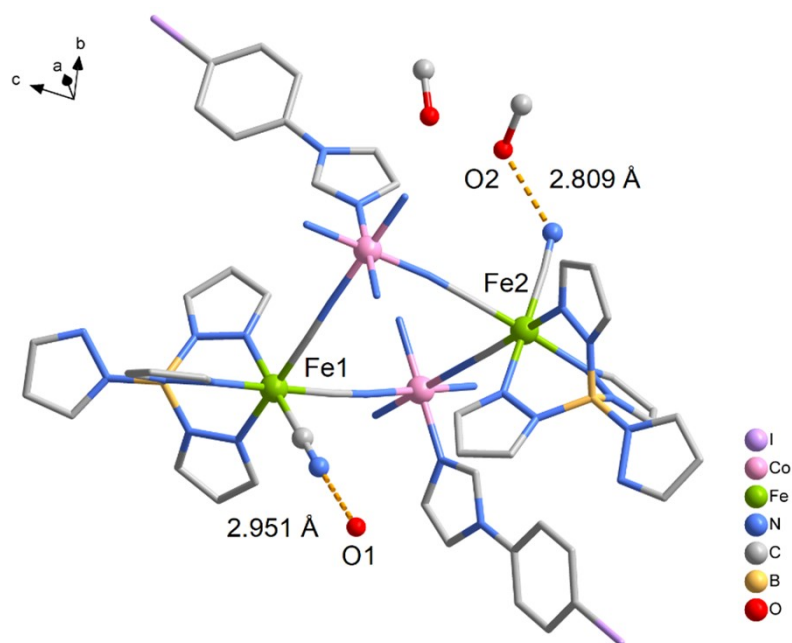


Fig. S13. Hydrogen bonds formed between lattice solvent molecules and terminal cyanide nitrogen atoms for **1·solv**. H atoms have been omitted for clarity. Color code: Co, pink; Fe, green; B, yellow; C, grey; N, blue; O, red; I, purple.

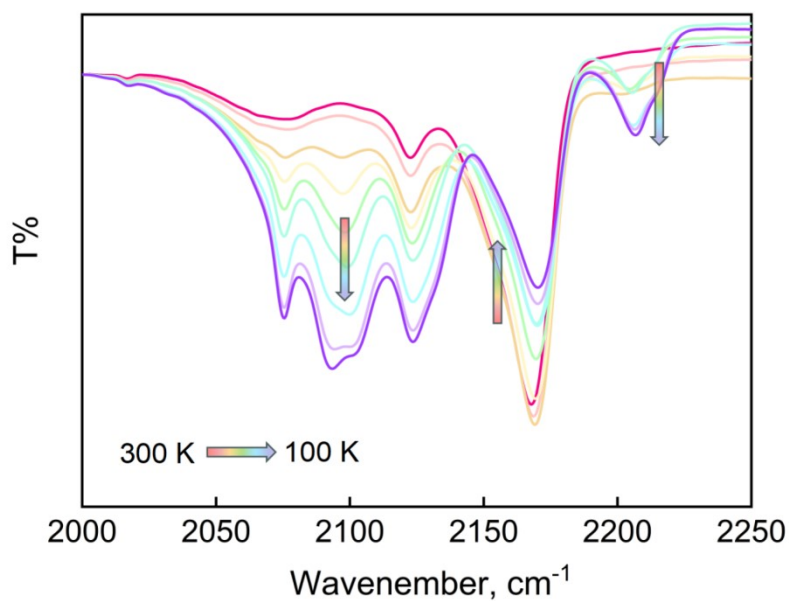


Fig. S14. Variable temperature solid state IR spectra of **1·desolv** in cooling mode.

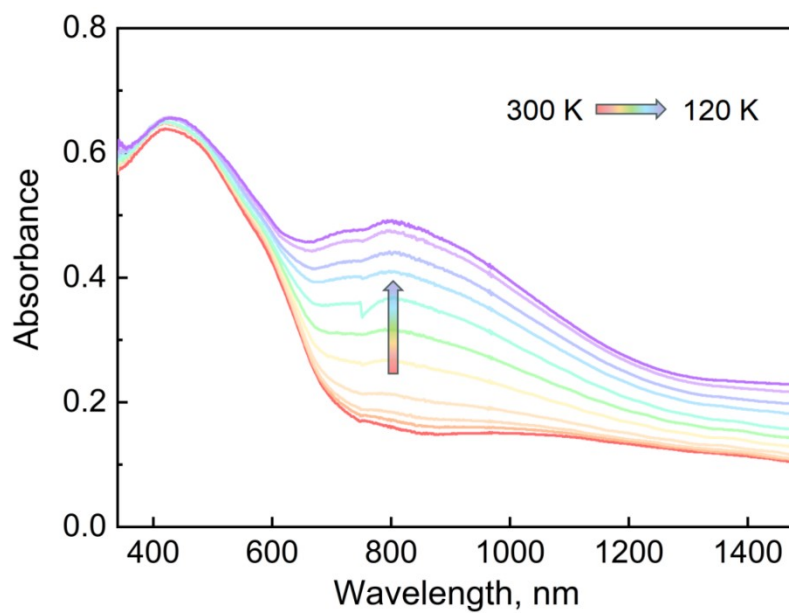


Fig. S15. Variable temperature solid state UV-vis-NIR absorption spectra of **1·desolv** in cooling mode.

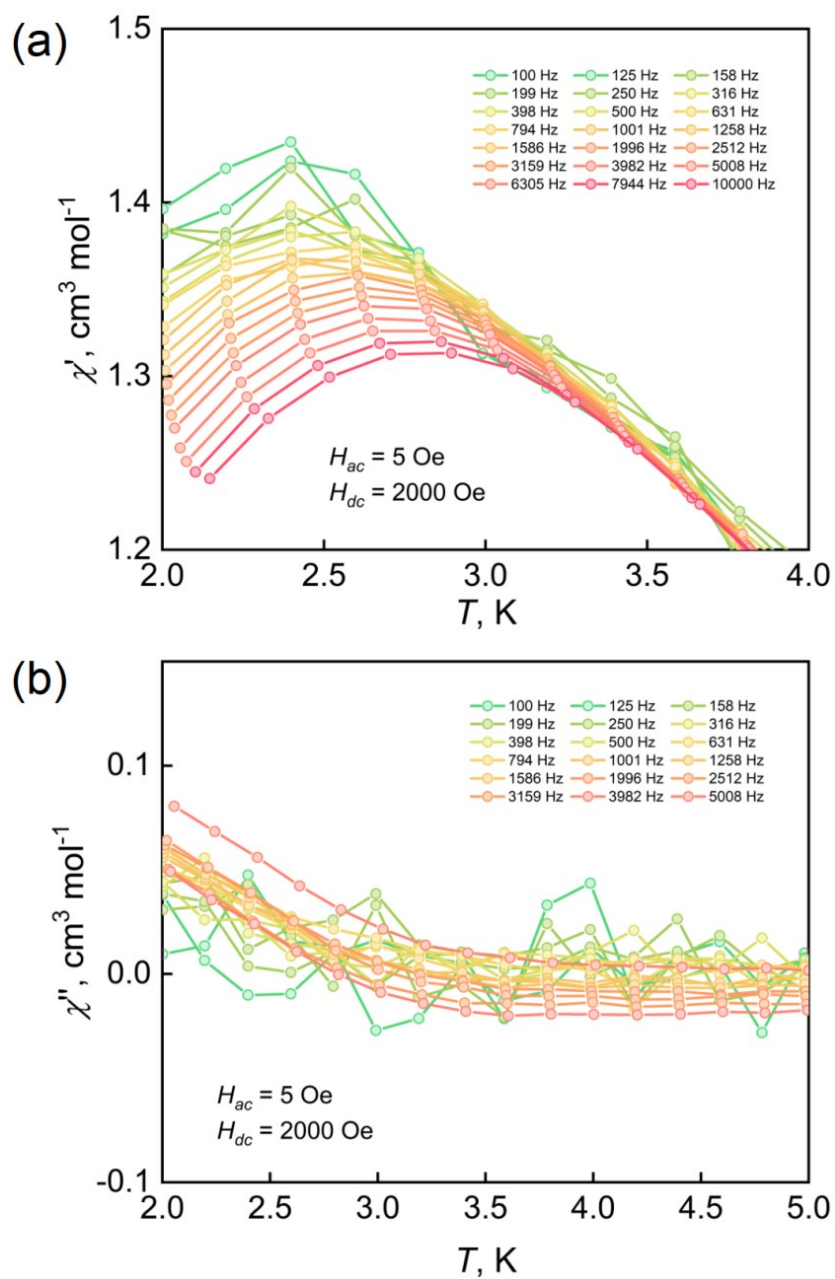


Fig. S16. Temperature dependence of in-phase signals (χ') (a) and out-of-phase signals (χ'') (b) for **1•desolv** under a 5 Oe AC field and 2000 Oe DC field.

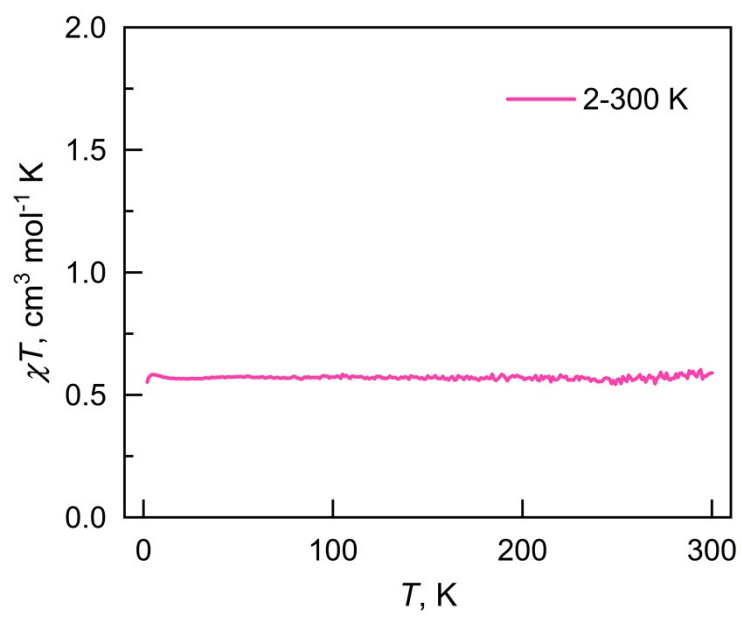


Fig. S17. Plots of χT vs. T for **1·resolv.**